Conformational dynamics of ATP/Mg:ATP in motor proteins via data mining and molecular simulation

A. Bojovschi,[a] Ming S. Liu,[b] and Richard J. Sadus[c]
Centre for Molecular Simulation, Swinburne University of Technology, P.O. Box 218, Hawthorn, Victoria 3122, Australia

(Received 20 April 2012; accepted 26 June 2012; published online 15 August 2012)

The conformational diversity of ATP/Mg:ATP in motor proteins was investigated using molecular dynamics and data mining. Adenosine triphosphate (ATP) conformations were found to be constrained mostly by inter cavity motifs in the motor proteins. It is demonstrated that ATP favors extended conformations in the tight pockets of motor proteins such as F_1-ATPase and actin whereas compact structures are favored in motor proteins such as RNA polymerase and DNA helicase. The incorporation of Mg^{2+} leads to increased flexibility of ATP molecules. The differences in the conformational dynamics of ATP/Mg:ATP in various motor proteins was quantified by the radius of gyration. The relationship between the simulation results and those obtained by data mining of motor proteins available in the protein data bank is analyzed. The data mining analysis of motor proteins supports the conformational diversity of the phosphate group of ATP obtained computationally. © *2012 American Institute of Physics*. [http://dx.doi.org/10.1063/1.4739308]

I. INTRODUCTION

Adenosine triphosphate (ATP) is the universal currency of energy in biological systems.[1] The structural conformation of ATP tightly coupled with its efficient hydrolysis is essential for the functionality of motor proteins.[2,3] Motor proteins are natural proteins that exert forces and motions at cellular levels. They produce the mechanics while fulfilling various biochemical functions.[4,5] For example, ATPase is an important class of motor proteins that converts chemical energy released from the hydrolysis of nucleotides (mainly ATP and its analogues) into mechanical functions. In addition to efficiently catalyzing ATP, ATPase systems have other important roles such as importing metabolites from the outer cell environment and releasing cellular wastes that can perturb the cell function.[1] Knowledge of the structural states of ATP (Refs. 6 and 7) and its coordination[8–10] by Mg^{2+} is important for our understanding of the functions of motor proteins. A detailed analysis of the role of ATP in specific motor proteins is also desirable for the therapeutic use of inhibition[11] efficient drug design[12,13] and the development of hybrid bio-nano-devices.[14–19]

The soluble part of F_0F_1-ATPase, known as F_1-ATPase[20] is possibly the most extensively-studied ATPase system. This protein works as a rotary molecular motor in which the γ-subunit rotates in relation to the surrounding $(\alpha\beta)_3$ subunits, while ATP is hydrolyzed on the three β-subunits. Its exceptional efficiency in transducing chemical energy to mechanics shows that F_1-ATPase is a potential nano-motor for various applications.[21,22] However, the operating mechanism and dynamics in F_1-ATPase is not totally clarified at the molecular level. For example, conformational dynamics and the binding/unbinding pathways of ATP molecules into the active subunits are only partially understood. Furthermore, the role of Mg^{2+} in coordinating the catalytic group and mechanical function of F_1-ATPase is not clear.

DNA helicase and RNA polymerase are motor proteins that move uni-directionally along the DNA strand.[23–25] DNA helicase has been shown to have a mixed motion composed of translations and rotations along the DNA.[26] The helical motion of helicases is driven by ATP hydrolysis.[27,28] Structural and biochemical studies have revealed the role of amino-acids and DNA binding on the hydrolysis of ATP in PcrA helicase.[29] Similar mechanochemistry in F_1-ATPase and PcrA helicase were reported previously.[30] The conformational changes of ATP in DNA helicase and its hydrolysis are correlated with the unwinding of DNA.[31,32] RNA polymerase uses the free energy of ATP binding and hydrolysis to propel itself along DNA and transcribe the information encoded in the gene sequences of DNA into RNA. The mechanisms that drive the translocation of RNA polymerase along DNA strand is not clear.[33]

The snapshots of ATP/Mg:ATP from the crystal structures of motor proteins in the protein data bank (PDB) (Ref. 34) provide a rich dataset of structural conformations. Molecular simulation is a powerful method to produce conformational dynamics of proteins at the molecular level.[35] In this work, conformational changes of ATP/Mg:ATP in motor proteins are assessed by data mining the crystal structures in comparison with molecular simulations. The conformational dynamics of ATP/Mg:ATP is simulated in different motor proteins such as F_1-ATPase, RNA polymerase, and DNA helicase. The structural states obtained from molecular dynamics are analyzed in comparison with those from crystal structures of motor proteins derived from the PDB. Data mining was

[a]Present address: School of Electrical and Computer Engineering, RMIT University, GPO Box 2476, Melbourne, Victoria 3001, Australia. Electronic mail: alexe.bojovschi@rmit.edu.au.
[b]Present address: CSIRO Mathematics, Informatics and Statistics, Private Bag 33, Clayton South 3169, Victoria, Australia. Electronic mail: ming.liu@csiro.au.
[c]Author for whom correspondence should be addressed. Electronic mail: rsadus@swin.edu.au.

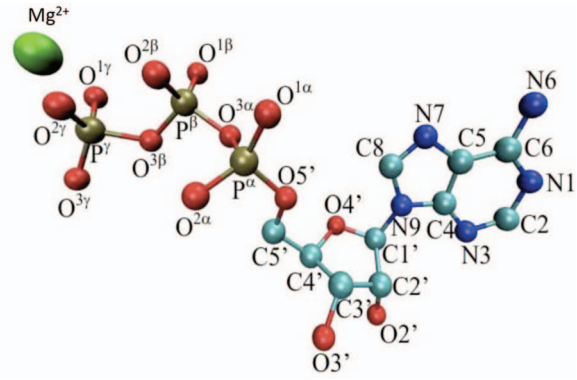

FIG. 1. Mg:ATP molecule with corresponding structure and atom names. The hydrogen atoms are not shown for clarity.

employed with the goal of identifying structural diversities of ATP/Mg:ATP phosphate group in crystal structures of motor proteins.

II. METHODS

A. Data mining of the crystal structures of ATP/Mg:ATP

Structural coordinates of ATP/Mg:ATP/Mg:ANP in motor proteins, including F_1-ATPase, actin, dynein, myosin, DNA helicase, DNA polymerase and RNA polymerase, were retrieved from the PDB. The ATP molecules were classified based on their presence in the catalytic or non-catalytic pocket and on the presence or absence of Mg^{2+} in the proximity of their phosphate group. The same treatment was applied for ANP (ATP analogue) that is present only in the crystal structures of F_1-ATPase. In this way, we identified and investigated a total of seven groups of motor proteins involving actin (52), RNA polymerase (6), DNA polymerase (4), myosin (2), F_1-ATPase (15), DNA helicase (3), and dynein (1). A list of all motor proteins investigated with the corresponding nucleotides in their enzymatic pocket is given in the supplementary materials.[36]

The structure of Mg:ATP with its corresponding atom designation is presented in Fig. 1. The conformational structures of ATP and Mg:ATP were analyzed and statistically translated via the distribution of inter-atomic distances and dihedral angles of the various atomic components. In this work, only the inter-atomic distance between P^{γ} and $C4'$ is presented. This was chosen as a dynamic descriptor of ATP structural changes. The data mining investigation provided useful insights on the conformational changes of ATP/Mg:ATP in motor proteins. Furthermore, the data mining results were used as a starting point for molecular dynamics simulations and to assess the simulation results.

B. Modeling motor proteins

In this work modeling and simulation were focused on F_1-ATPase, RNA-polymerase, and DNA helicase systems, e.g., fully solvated atomistic structure of motor proteins with ATP/Mg:ATP in their catalytic pockets. Visual molecular dynamics (VMD) (Ref. 37) was used to: (a) build the simulated systems; (b) check for steric clashes; (c) analyze the simulation trajectory; and (d) perform structural analyses. The Corey, Pauling and Koltun (CPK) space filling molecular model[38] was used for representing the atomic structure of Mg:ATP.

TABLE I. Simulations of motor proteins in solvent carried out in this work at 300 K using an integration time step of 1fs.

System name	Number of atoms	Boundary conditions
ATP in $\alpha\beta$ subunits of F_1-ATPase	132 991	PBC
ATP in RNA polymerase	42 909	PBC
Mg:ATP in $\alpha\beta$ subunits of F_1-ATPase	68 136	SBC
Mg:ATP in DNA helicase	54 385	SBC

C. Molecular simulation of ATP/Mg:ATP with different boundary conditions

All-atom molecular dynamics (MD) was used to characterize the dynamics of ATP/Mg:ATP in motor proteins (as summarized in Table I). All simulations were performed using NAMD 2.6 (Refs. 39 and 40) with the CHARMM 22-27 (Chemistry at Harvard Molecular Mechanics) force field.[41–43] NAMD in tandem with CHARMM has proven to perform well for investigating large biomolecular systems.[44] The structural parameters, interaction forces, and specific charges of ATP are defined in the CHARMM force field via the parameter and topology files. The TIP3P model was used for water molecules in all our MD simulations.[45] Every biomolecular system was firstly minimized and annealed. A depth first search method implemented in NAMD was used to minimize the system. An annealing protocol was used to avoid distortion of the system caused by a thermal jump from the minimization temperature of 0 K to the equilibration temperature of 300 K. This involved increasing the temperature of the system form 0 K to 300 K in steps of 25 K/1000 ps. The systems were equilibrated using MD simulations that included constant temperature control via Langevin dynamics (LD).

The velocity Verlet algorithm[46] was used for integrating the equations of motion. The bonds exclusion mechanism was employed to exclude certain pairs of atoms from electrostatic and van der Waals computation because of the interaction between bonded atoms. The cut-off distance was set to 14 Å for long-range interactions. A switching function of 12 Å was used to smoothly reduce the forces and energies to zero at the cut-off distance. All the systems were investigated with periodic boundary conditions (PBC) and spherical boundary conditions (SBC). The actual size of solvent sphere or solvent box was sufficiently large to allow Mg:ATP to move freely without reaching the boundaries cut-off distance. The simulations were performed from 2 ns up to 14 ns for DNA helicase. No difference in dynamics was found for simulations preformed with PBC and SBC. Typically, MD simulations were run in an NVT ensemble for at total of two million time 1 fs steps after an energy minimization period of 1000 time steps and

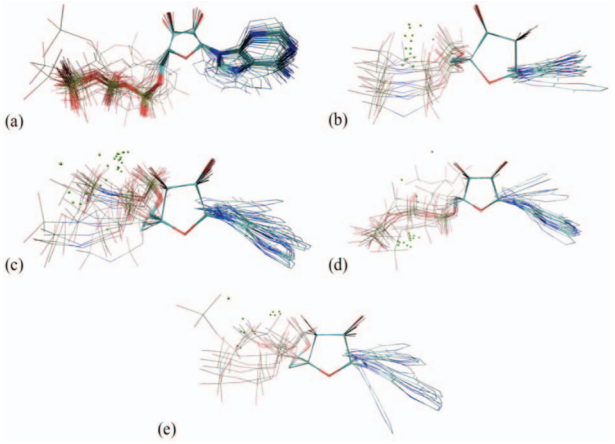

FIG. 2. Alignment of ATP/Mg:ATP/Mg:ANP using the ribose ring as the alignment reference. Results shown are the alignment of (a) 63 ATP from catalytic pockets; (b) 26 Mg:ANP from catalytic pockets; (c) 37 Mg:ANP from the non catalytic pockets; (d) 20 Mg:ATP from catalytic pockets and (e); 13 Mg:ATP from non catalytic pockets.

annealing of the molecular systems. This work presents the results obtained at the temperature of 300 K.

III. RESULTS AND DISCUSSION

A. Alignment of ATP/Mg:ATP molecules from motor proteins

The conformational diversity of both the phosphate group and adenine in ATP/Mg:ATP/Mg:ANP was studied by performing alignment analysis. Crystal structures of the ATP/Mg:ATP/Mg:ANP molecules from various motor proteins were aligned and superimposed using the ribose base ring as reference. The structures from catalytic and non-catalytic pockets of the 137 systems were aligned separately considering also the Mg^{2+} coordination as shown in Figs. 2(a)–2(e). The alignment results suggest that ATP and Mg:ATP/Mg:ANP are flexible and can undertake a large variety of conformational states in motor proteins. The phosphate group exhibits a widely distributed spatial configuration. When Mg^{2+} ions are absent, the negative charge of the phosphate groups of ATP are neutralized by positive tethers of amino acids (such as Arg, Lys, and His) from the binding pockets. Structural diversity is much more prominent in the presence of Mg^{2+}. Considerable conformational diversity of the phosphate group and adenine (as aligned against the ribose base) is also apparent from the simulation results presented in Figs. 3(a)–3(d). The presence of Mg^{2+} triggers conformational changes of the phosphate group that lead to structural changes of the ribose base.

The structural changes triggered by the presence of Mg^{2+} have a critical impact on the hydrolysis of ATP. Figures 3(a) and 3(b) indicate that ATP adopts conformations characterized by high fluctuations of the phosphate group and smaller more defined structural orientations of the adenine. These correspond to ATP structures obtained from simulations in $\alpha\beta$ subunits of F_1-ATPase and of RNA polymerase. When Mg:ATP is simulated in $\alpha\beta$ subunits of F_1-ATPase and in DNA helicase it can be observed that adenine adopts two distinct orientations (Figs. 3(c) and 3(d)). The conformational changes in the presence of Mg^{2+} coordination are more evident if the structures are rotated by 90°. It can be noted that the different orientations of the ribose ring correspond to different orientations of adenine and phosphate group. The data used in Fig. 3 were obtained from 2 ns simulations with a structure extracted at every 5000 timestep.

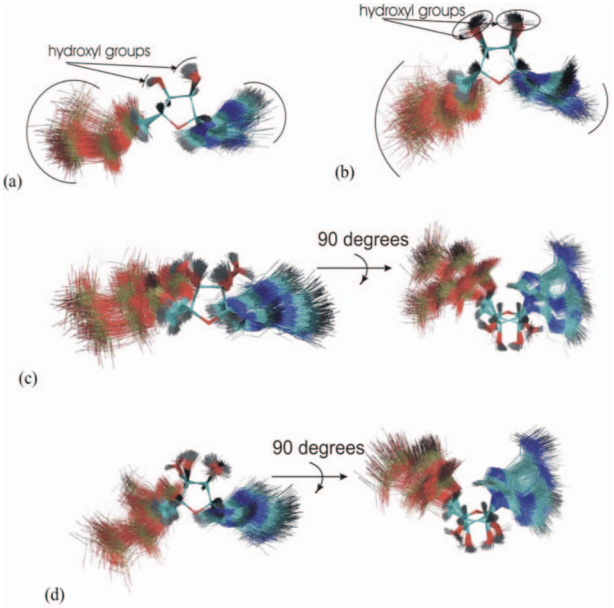

FIG. 3. Alignment of 400 ATP/Mg:ATP molecules on their ribose ring. Results are shown for the alignment of (a) ATP structures simulated in $\alpha\beta$ (BF segments) subunits of F_1-ATPase; (b) ATP structures simulated in RNA polymerase; (c) Mg:ATP structures simulated in $\alpha\beta$ subunits (BF segments) of F_1-ATPase; and (d) Mg:ATP structures simulated in DNA helicase. The structural changes of ribose ring are shown by a side view.

The structural orientation of ATP is essential in the catalytic process. The results show that besides its critical role in cleaving the phosphate bond of the γ- phosphate, Mg^{2+} plays a role in the structural orientation of ATP in motor proteins. This observation is in agreement with the experimental results presented in Fig. 2. Further details regarding the Mg^{2+} coordinating roles can be found in the supplementary material.[36]

B. Distance constraint in ATP/Mg:ATP

The conformational flexibility of the phosphate group of ATP/Mg:ATP was explored from results obtained by simulating ATP/Mg:ATP in RNA polymerase, DNA helicase and F_1-ATPase motor proteins. The inter-atomic distance between P^{γ} and C4' is presented in Fig. 4 for this purpose. Measurements of this distance revealed that the conformational changes in ATP/Mg:ATP/Mg:ANP are conserved. However ATP in the absence of Mg^{2+} adopts more extended structures than in the presence of Mg^{2+}. As shown in Fig. 4, in the absence of Mg^{2+} this inter-atomic distance peaks at about 7.75 Å whereas in the presence of Mg^{2+} the same inter atomic distance peaks at a value of about 7.5 Å. The possible values of this inter atomic distance as can be seen from the crystal structure investigations, span from 6 Å up to 8.4 Å. The results show that this inter atomic distance difference is not only due to the presence

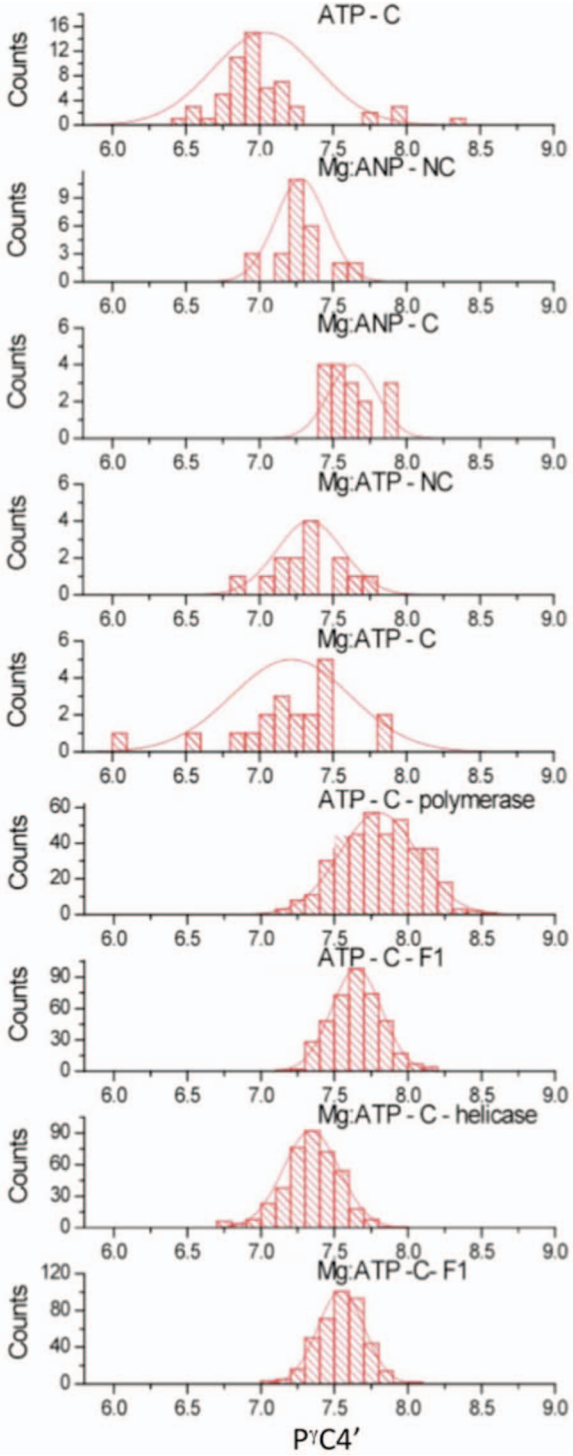

FIG. 4. Distribution of the distance between P$^{\gamma}$ and C4′ atoms of ATP/ANP. Results are shown separately for ATP/ANP in catalytic (C) and non-catalytic (NC) pockets in both the absence (labeled as ATP) or presence (labeled as Mg:ATP/Mg:ANP) of Mg^{2+} coordination. In the top five diagrams the P$^{\gamma}$C4' inter atomic distance is from crystal structures, whereas the remaining data are from simulations. ATP was simulated in the $\alpha\beta$ (BF segments) subunits of F_1-ATPase, or DNA helicases or RNA polymerase. The line signifies a Gaussian distribution.

or absence of Mg^{2+} but also depends on the state of the ATP binding pocket (open or closed), the surrounding amino acids and the number of water molecules present in the pocket.

It is understood that Mg^{2+} dynamically coordinates, mainly via the bonding networks with the oxygen atoms, the beta or gamma phosphates and amino acids in the pocket. Investigations of the distance between Mg^{2+} and oxygen atoms from the phosphate region indicate that Mg^{2+} is communally coordinating α-, β-, and γ-phosphate or α- and γ-phosphate in loose pockets of motor proteins and in solvent, but Mg^{2+} only tackles β- and γ-phosphate in the tight pockets of motor proteins. The crystal structure analysis of motor proteins shows that, when two or three oxygen atoms from these phosphate groups coordinate Mg^{2+}, the inter-atomic distance is varying from 1.8 Å to 2.93 Å.[36]

C. Radius of gyration for ATP/Mg:ATP in different motor proteins

The flexibility and particularly the degree of extensibility of ATP/Mg:ATP were assessed by the radius of gyration. Analysis of radius of gyration of ATP in crystal structures was performed separately for the catalytic and non-catalytic pocket and in the presence and absence of Mg^{2+} coordination, respectively. Alignment results showed that Mg^{2+} enhances the structural flexibility of ATP. The extensibility of ATP molecules is a reflection of the conformational structure of the pocket. The extent to which the pocket is open or closed has an important role on the conformation of ATP. Moreover the amino acids that surround the ATP in the pocket have a localized effect on ATP and determine its structural conformation. Crystal investigations show that, in the absence of Mg^{2+}, ATP has the most extended structures in actin followed by RNA polymerase, dynein and DNA helicase (Fig. 5(a)).

The degree of extensibility of ATP can be mostly assessed in actin and F_1-ATPase, for which a large number of crystal structures with ATP bound are available. For the other motors, the number of structures available does not allow statistical interpretation of the extensibility of ATP. Comparing Fig. 5(a) with Fig. 5(b) it is apparent that the highest values for the radius of gyration are obtained for ATP from crystal structures in the presence of Mg^{2+}. The average value is ~5.1 Å for ATP in the catalytic pocket of actin motor without Mg^{2+} and ~5.2 Å with Mg^{2+}. The investigation of the radius of gyration in crystals with Mg^{2+} revealed that extended structures were mainly present in actin motors, medium extended structures in F_1-ATPase, DNA helicase and dynein motors, while less extended structures were present in myosin and RNA polymerase motors (Fig. 5(b)).

Although the number of crystal structures is not as large to provide an exclusive conclusion of the extensibility of ATP in motor proteins, it provides solid information for the diversity of conformational states. These results and the detailed structure analysis of different motor proteins suggest that ATP adopts less extended structures in tight pockets, as well as in pockets where there are a number of water molecules surrounding the nucleotide. In Figs. 5(a) and 5(b) there is little difference between the degrees of extensibility of ATP in catalytic and non-catalytic pocket. This is further illustrated in Fig. 5(c), which compares the mean and standard deviation of the radius of gyration of ATP and ANP from crystal structures of motor proteins. The main dynamics differences are for the mean values of ATP in the catalytic pockets either in the presence or absence of Mg^{2+} coordination. These are

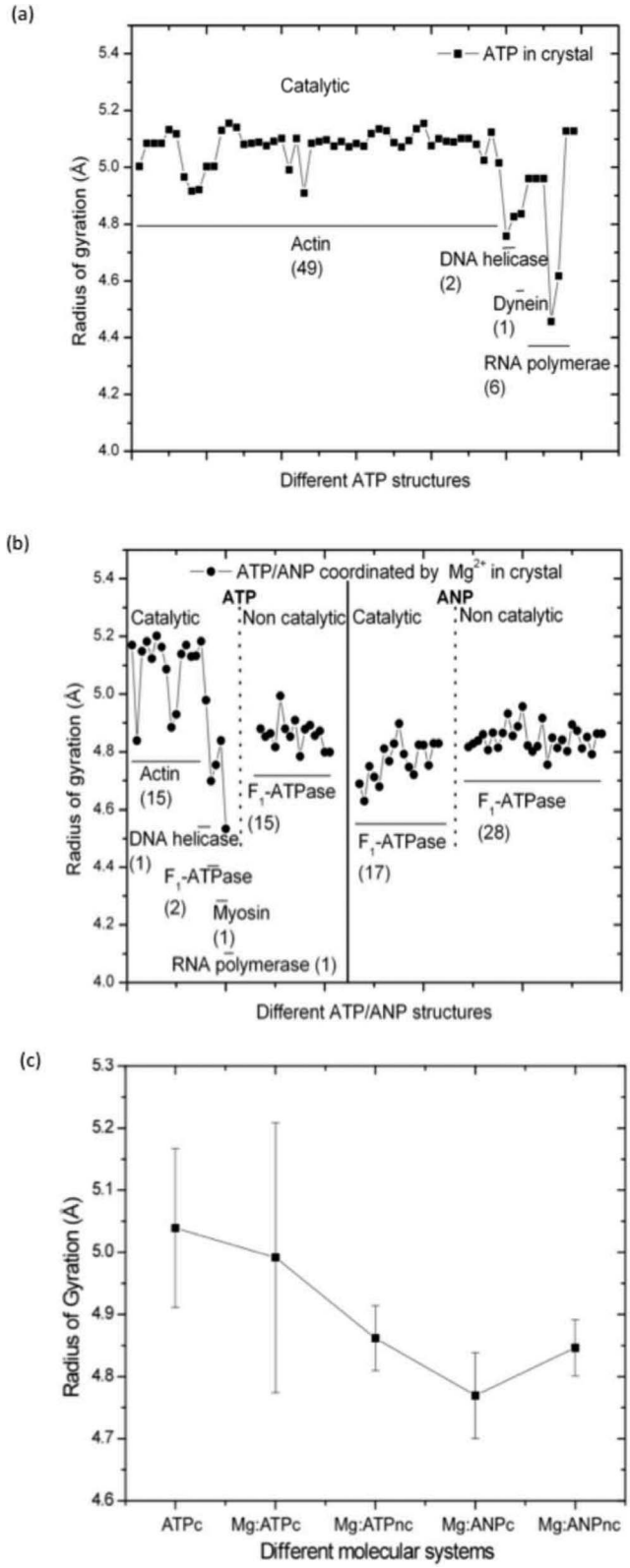

FIG. 5. Radius of gyration for ATP and ATP/ANP coordinated by Mg^{2+} in catalytic and non-catalytic pockets. The values in brackets represent the number of ATP/ANP crystal structures used. Results are shown for (a) ATP structures extracted from the catalytic pocket of motor proteins; (b) ATP/ANP structures extracted from the catalytic and non-catalytic pocket of motor proteins; and (c) average values and standard deviations for the data presented in (a) and (b). ATP/ANP are coordinated by Mg^{2+} in their pocket and the results are divided in two parts by a solid line. ATP values are given to the left of the line, whereas ANP results are to the right. In both cases a dashed line separates catalytic and non-pocket data.

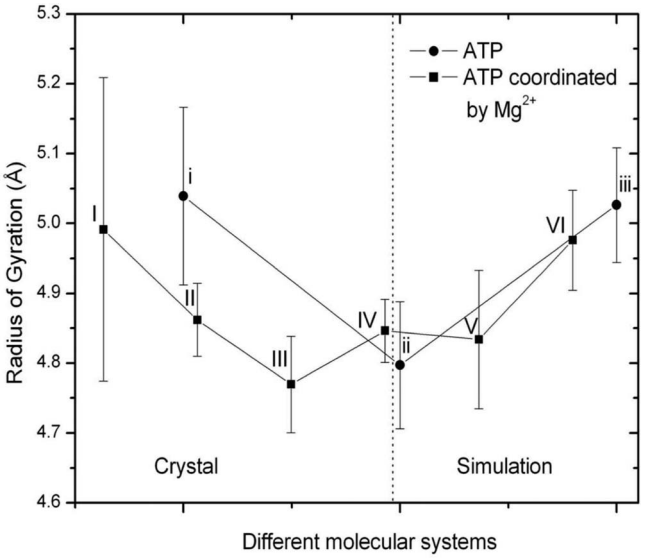

FIG. 6. Comparison of the average radius of gyration for ATP from crystal structure and from simulation (separated by a dashed line). The averaged values for ATP correspond to (i) the catalytic region of crystal structures of motor proteins; (ii) simulated in the RNA polymerase (PDB : 1HI1); and (iii) simulated in $\alpha\beta$ (BF segments) catalytic region of F_1-ATPase (PDB: 1H8H) (note: Mg^{2+} was removed manually from the pocket before simulation). For the case of Mg^{2+} coordinating ATP/ANP results are shown for ATP in both catalytic (I) and non-catalytic (II) pockets and ANP from catalytic (III) and non-catalytic (IV) regions of crystal structures of motor proteins. Values are also given for ATP simulated in DNA helicase (PDB : 1QHG) (V); and $\alpha\beta$ (BF segments) catalytic region of F_1-ATPase (PDB: 1H8H) (VI).

reflected in the different conformations adopted by ATP in actin, DNA helicase, dynein and RNA polymerase. The behavior of Mg:ATP in water and its elastic properties have been previously reported.[47] However, this work brings quantitative insights to Mg:ATP conformational dynamics and their extensibility in motor proteins by interpreting the radius of gyration.

To provide a better understanding of the degree of the extensibility of ATP in motor proteins, we further compared the radius of gyration from the simulation results of four systems (Table I) with the corresponding crystal structures. The results are plotted along with the radius of gyration obtained from crystal structures as shown in Figure 6. Smaller values of the radius of gyration for ATP in RNA polymerase and DNA helicase are due to their pocket structure which does not confine the nucleotide in the same extend as $\alpha\beta$ subunits from F_1-ATPase does. This allows water molecules to easily diffuse into the pocket and force ATP/Mg:ATP to adopt a much more compact structure. The simulation results show that the degree of extensibility of ATP/Mg:ATP is smaller in the presence of solvent. Also ATP/Mg:ATP in solvent indicated that the average value of the radius of gyration is smaller then in any protein investigated.[36] The presence of a small number of water molecules in the pocket leads to relatively extended structures of ATP. Mg^{2+} shields partially the negative charges of the phosphate group and reduces its extensibility by coordinating mechanisms. As shown in inter-atomic distance results presented in Sec. III B, the distance between P^{γ} and $C4'$ is smaller in the presence of Mg^{2+}. This inter atomic difference was reflected also in the radius of gyration. In

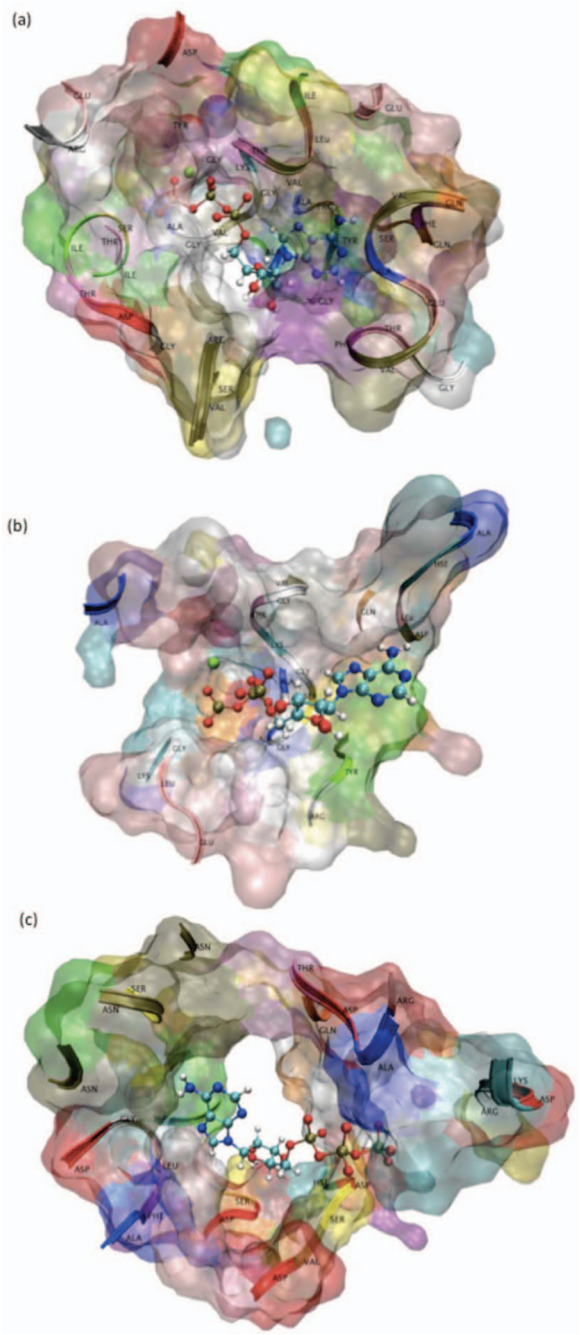

FIG. 7. The protein within 8 Å of ATP/Mg:ATP extracted from (a) $\alpha\beta$ (BF segments) subunits of F_1-ATPase; (b) DNA helicase; and (c) RNA polymerase. It can be observed that $\alpha\beta$ subunits (BF segments) of F_1-ATPase surround ATP representing a closed state of the F_1-ATPase binding pocket while RNA polymerase and DNA helicase are open pockets.

Fig. 6, the radius of gyration of ATP in the absence of Mg^{2+} in $\alpha\beta$ subunits of F_1-ATPase is also found to be larger than in the presence of Mg^{2+}.

D. Backbone dynamics in molecular motors

The structural fluctuation of a ligand in different pockets depends on the dynamic changes of the pocket. In Fig. 7 ATP structural conformations in the pockets of different molecular motors are illustrated. In the $\boldsymbol{\alpha\beta}$ subunits of F_1-ATPase (Fig. 7(a)) the fluctuations of ATP are much constrained compared with the case in DNA helicase and RNA polymerase (Figs. 7(b) and 7(c)). The open nature of the ATP pocket in DNA helicase and RNA polymerase and the presence of water molecules allow ATP to undergo more fluctuations. This is shown in Fig. 9 using root mean square fluctuation (RMSF) for ATP simulated in F1-ATPase and RNA polymerase. There is an intrinsic relation between the conformational changes of a ligand and the backbone of an enzyme.

Given that the RMSF of the atoms can characterise the dynamical stability of a molecular system, we calculated RMSFs of C$\boldsymbol{\alpha}$ atoms for molecular motors and compared with the values obtained using the temperature factors of the same crystal structure. The fluctuations of the crystal structure expressed by the experimental B-factor were converted to RMSF values.[36] In Fig. 8, the RMSF obtained from simulations agree very well with the RMSF obtained from the crystal structure of the same systems. There are only a few residues for which RMSF obtained from simulations differs slightly from that obtained from crystal. These residues correspond mainly to solvent exposed residues and loop regions, which are characterised by greater flexibility. In Fig. 8(a) it can be observed that the main difference is for the terminal regions of $\boldsymbol{\alpha}$ and $\boldsymbol{\beta}$ subunits. The buried residues and beta-strands have smaller values of RMSF. The RMSF calculated for RNA polymerase (Figure 8(b)) in solvent is similar with RMSF obtained from the B-factor of crystal structures. Good agreement between experimental results and those from simulations is shown in Figure 8(c) for DNA helicase. The RMSF results show that the structural dynamics of the molecular motors simulated are in agreement with the experiments. This is critical for ensuring that the nucleotide structure experiences realistic constraints.

E. Nucleotide pocket interaction

The pair interaction energy governs the stability and dynamics of the molecular systems. In this work the pair interaction energy was calculated to quantify the strength of connectivity between ATP and both the binding pocket and the water molecules that diffused in the pocket. For calculating the pair interaction energy, the region of protein/water molecules within 8 Å of ATP was chosen (as illustrated in Fig. 7), where the water molecules are not drawn for clarity. The strength of interaction between the nucleotide and the catalytic pocket is diminished by the diffusion of water in the pocket. The diffusion of water depends on the geometry of the catalytic pocket and the surrounding amino-acids. It was shown in Fig. 7(a) that ATP in $\alpha\beta$-subunits of F_1-ATPase is confined by the surrounding amino-acids from the catalytic pocket. In an 8 Å sphere around ATP there are 77 amino-acids in $\alpha\beta$-subunits of F_1-ATPase, 49 amino-acids in DNA helicase and 49 amino-acids in RNA polymerase. The amino acids and specific motor proteins are summarized in the supplementary matetials.[36] In DNA helicase (Fig. 7(b)) and RNA polymerase (Fig. 7(c)) the structure of the pocket is more open and allows water molecules to diffuse easily in the pocket. This results in an increase of the pair interaction energy between ATP and the surrounding amino-acids. In Fig. 10 it can

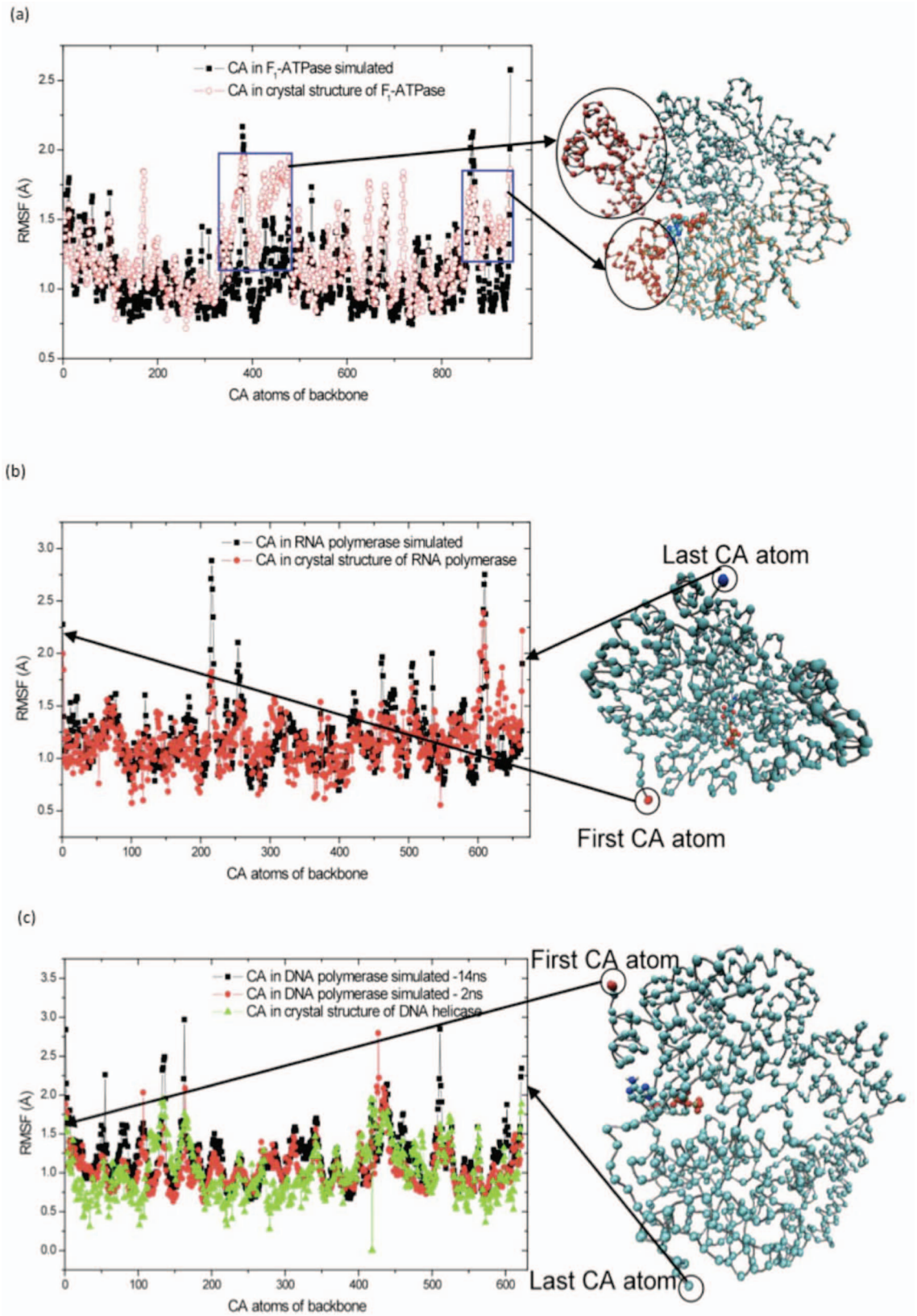

FIG. 8. Comparison of RMSF values obtained from crystal with simulation data. RMSFs are shown for the Cα atoms of (a) $\alpha\beta$ subunits of F_1-ATPase; (b) RNA polymerase and (c) DNA helicase.

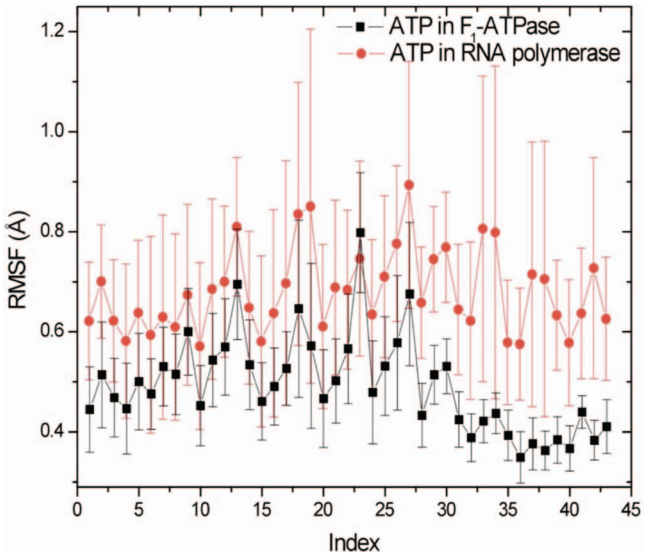

FIG. 9. RMSF of ATP in $\alpha\beta$ subunits of F_1-ATPase and in RNA polymerase The indexes of the atoms from 1 to 42 correspond to the atom names in the following order C4′, H4′, O4′, C1′, H1′, C5′, N7, C8, H8, N9, N1, C2, H2, N3, C4, 15 is C6, N6, H61, H62, C2′, H2″, O2′, H2′, C3′, H3′, O3′, H3T, C5′, H5′, H5″, O5′, P^{α}, $O^{1\alpha}$, $O^{2\alpha}$, $O^{3\alpha}$, P^{β}, $O^{1\beta}$, $O^{2\beta}$, $O^{3\beta}$, P^{γ}, $O^{1\gamma}$, $O^{2\gamma}$, and $O^{3\gamma}$. The standard deviation was calculated from 10 different simulations.

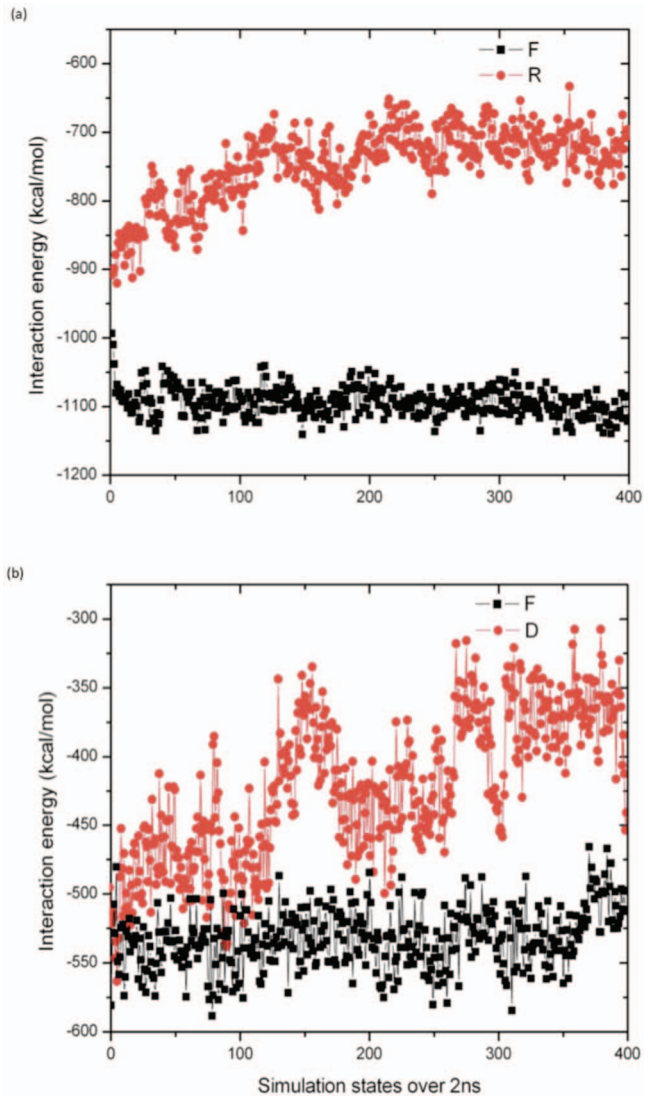

FIG. 10. The pair interaction energy between ATP and the protein that surrounds the molecule in a 8 Å radius. Results are shown for ATP in (a) RNA polymerase (R) and in $\alpha\beta$ (BF segments) subunits of F_1-ATPase (F); and Mg:ATP in (b) DNA polymerase (D) $\alpha\beta$ (BF segments) subunits of F_1-ATPase (F).

be observed that the pair interaction energy between ATP and the pocket is higher in the RNA polymerase in comparison with the pair interaction energy between ATP and the $\alpha\beta$-subunits from F_1-ATPase. The value of pair interaction energy between ATP and the amino-acids within 8Å of ATP in RNA polymerase increases from approximately −900 kcal/mol towards an equilibrium value of approximately −750 kcal/mol. The equilibrium value is reached when water molecules take all the available space in the pocket and no further diffusion of water molecules is possible. The pair interaction energy between ATP and the pocket region defined by proteins within 8 Å of ATP in F_1-ATPase is also presented in Figure 10. The equilibrium value for the pair interaction energy in this case is approximately −1100 kcal/mol.

The same behavior is obtained from the investigation of Mg:ATP in DNA helicase and $\alpha\beta$-subunits of F_1-ATPase. The difference is that the number of water molecules that diffuse in the DNA helicase catalytic pocket is smaller. The effect of this can be seen in a larger radius of gyration of ATP in DNA helicase compare with RNA polymerase as shown in Sec. III C. This is translated energetically in a smaller difference between the pair interaction energy between ATP and the protein within 8 Å of ATP in DNA polymerase and $\alpha\beta$-subunits of F_1-ATPase (Fig. 10(b)). The pair interaction energy between ATP and the amino-acids within 8 Å of ATP reaches an equilibrium value of approximately −375 kcal/mol in DNA helicase and approximately −525 kcal/mol in $\alpha\beta$-subunits of F_1-ATPase. The presence of Mg^{2+} plays a shielding effect determining the value of the pair interaction energy to be higher than in Fig. 10(a). Mg^{2+} was not counted in the pair interaction energy calculations. The fluctuations of the pair interaction energy describe the dynamics of the water molecules in the pocket. The pair interaction energy reaches a plateau value when the water molecules equilibrate in the pocket and Mg^{2+} has a stable coordinating state. In addition to their role in defining the conformational dynamics of ATP, the water molecules are also crucial for catalysis. This understanding of the interaction mechanisms between ions, water, nucleotide and protein is essential in drug design and for fostering the motor proteins in nanotechnological applications.

The pair interaction energy between ATP and the water molecules within 8 Å of ATP that diffused in the pocket was also investigated (Fig. 11). The pair interaction energy between ATP and water molecules reaches equilibrium in RNA polymerase at a value of approximately −800 kcal/mol after an evident decrease from −300 kcal/mol. In the $\alpha\beta$-subunits of F_1-ATPase the equilibrium value was reached at approximately −150 kcal/mol (Fig. 11(a)). In the presence of Mg^{2+} the pair interaction energy between ATP and water within 8 Å of ATP is approximately −375 kcal/mol in DNA helicase and

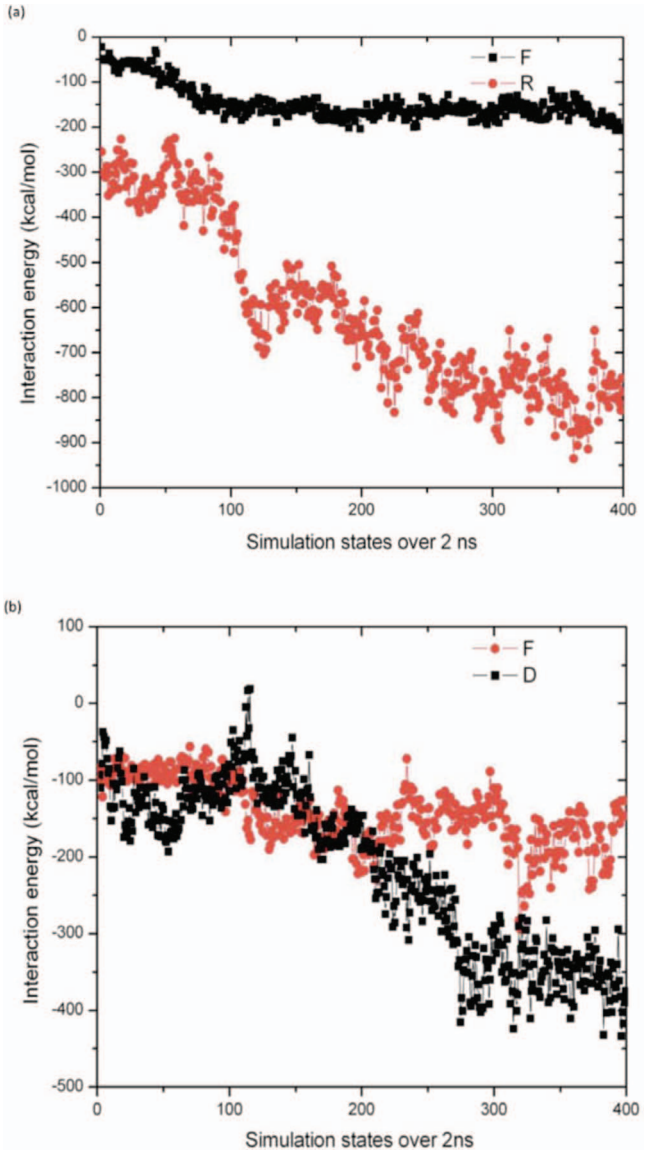

FIG. 11. The pair interaction energy between ATP and the water that surrounds the molecule in a 8 Å radius. Results are shown for ATP in (a) RNA polymerase (R) and in $\alpha\beta$ (BF segments) subunits of F_1-ATPase (F); and Mg:ATP in (b) DNA polymerase (D) $\alpha\beta$ (BF segments) subunits of F_1-ATPase (F).

−150 kcal/mol in $\alpha\beta$-subunits of F_1-ATPase (Fig. 11(b)). The average number of water molecules around ATP in a sphere of radius 8 Å is 26 for F_1-ATPase, 117 for DNA helicase, and 100 for RNA polymerase. We showed that the pair interaction energy could be correlated also with the density of water molecule in the pocket and with the catalytic favorable states of ATP in the motor proteins.[36]

IV. CONCLUSIONS

The conformational diversity of ATP/Mg:ATP in motor proteins was studied via data mining of crystal structures in conjunction with molecular simulation. The combined molecular simulation and data mining investigations provide a detailed picture of conformational dynamics of ATP/Mg:ATP in molecular motors.

Alignment data of 159 nucleotides shows the wide variety of conformational states expressed in motor proteins. The probability of distribution analysis of the distance between P^{γ} and C4' atoms of the nucleotides in the absence of Mg^{2+} peaks at about 7.75 Å whereas in the presence of Mg^{2+} the same inter atomic distance peaks at a value of about 7.5 Å. The results show that this difference in inter atomic distance is due to Mg^{2+}, the state of the ATP binding pocket, the surrounding amino acids that are specific to each motor protein, and the number of water molecules present in the pocket.

The radius of gyration analysis indicated that in motor proteins ATP can have compact structures and extended structures with a radius of gyration as small as 4.43 Å and, respectively, as large as 5.2 Å. RMSF values of the Cα atoms of the backbone of the motor protein investigated are between 0 Å and 3 Å. The average value of RMSF for Cα of about 1 Å indicates the stability of the structures. The values of temperature factors derived from RMSF obtained from simulations are in good agreement with those from experiments.

The pair interaction energy between ATP and the amino-acids within 8 Å of ATP at equilibrium in presence of Mg^{2+} is −375 kcal/mol in DNA helicase and −525 kcal/mol in $\alpha\beta$-subunits of F_1-ATPase, respectively. In the absence of Mg^{2+} the values of the interaction energies are lower, which is probably due to the absence of Mg^{2+} shielding. The pair interaction energy between water molecules, which modulate the conformational changes of ATP, also show a consistent correlation to water density in the binding pockets.

ACKNOWLEDGMENTS

We thank the Victoria Partnership for Advanced Computing (VPAC) and the National Computational Infrastructure (NCI) for generous allocations of computing resources. A.B. thanks Swinburne University of Technology for a postgraduate scholarship.

[1]D. L. Nelson and M. M. Cox, *Lehninger Principles of Biochemistry* (Freeman, 2005), Vol. 708, Chap. 19.
[2]M. S. Liu, B. D. Todd, and R. J. Sadus, Biochim. Biophys. Acta **1752**, 111 (2005).
[3]E. Pebay-Peyroula, C. Dahout-Gonzalez, R. Kahn, V. Trezeguet, G. J. Lauquin, and G. Brandolin, Nature (London) **426**, 39 (2003).
[4]M. Schliwa and G. Woehlke, Nature (London) **422**, 759 (2003).
[5]P. D. Boyer, Nature (London) **402**, 247 (1999).
[6]T. V. Pyrkov, Y. A. Kosinsky, A. S. Arseniev, J. P. Priestle, E. Jacoby, and R. G. Efremov, Proteins **66**, 388 (2007).
[7]G. R. Stockwell and J. M. Thornton, J. Mol. Biol. **356**, 928 (2006).
[8]A. S. Mildvan, Magnesium **6**, 28 (1987).
[9]J. Weber, S. T. Hammond, S. Wilke-Mounts, and A. E. Senior, Biochemistry **37**, 608 (1998).
[10]Y. H. Ko, S. J. Hong, and P. L. Pedersen, J. Biol. Chem. **274**, 28853 (1999).
[11]E. Perola and P. S. Charifson, J. Med. Chem. **47**, 2499 (2004).
[12]P. Chene, Nat. Rev. Drug Discovery **1**, 665 (2002).
[13]L. Mao, Y. Wang, Y. Liu, and X. Hu, J. Mol. Biol. **336**, 787 (2004).
[14]P. Guo, Methods Mol. Biol. **300**, 285 (2005).
[15]H. Hess, J. Clemmens, D. Qin, J. Howard, and V. Vogel, Nano Lett. **1**, 235 (2001).
[16]H. Liu, J. J. Schmidt, G. D. Bachand, S. S. Rizk, L. L. Looger, H. W. Hellinga, and C. D. Montemagno, Nature Mater. **1**, 173 (2002).
[17]Z. Yinghao, W. Jun, C. Yuanbo, Y. Jiachang, and F. Xiaohong, Biochem. Biophys. Res. Commun. **331**, 370 (2005).
[18]M. Knoblauch, G. A. Noll, T. Muller, D. Prufer, I. Schneider-Huther, D. Scharner, A. J. Van Bel, and W. S. Peters, Nature Mater. **2**, 600 (2003).

[19]C. Mavroidis, A. Dubey, and M. L. Yarmush, Annu. Rev. Biomed. Eng. **6**, 363 (2004).
[20]M. E. Pullman, H. S. Penefsky, A. Datta, and E. Racker, J. Biol. Chem. **235**, 3322 (1960).
[21]K. Kinosita, Jr., R. Yasuda, H. Noji, and K. Adachi, Phil. Trans. R. Soc. Lond. B **355**, 473 (2000).
[22]M. S. Liu, B. D. Todd, and R. J. Sadus, J. Chem. Phys. **118**, 9890 (2003).
[23]L. Bai, T. J. Santangelo, and M. D. Wang, Annu. Rev. Biophys. Biomol. Struct. **35**, 343 (2006).
[24]A. Shilatifard, R. C. Conaway, and J. W. Conaway, Annu. Rev. Biochem. **72**, 693 (2003).
[25]E. Jankowsky, Nature (London) **437**, 1245 (2005).
[26]C. Doering, B. Ermentrout, and G. Oster, Biophys. J. **69**, 2256 (1995).
[27]S. S. Patel, M. M. Hingorani, and W. M. Ng, Biochemistry **33**, 7857 (1994).
[28]S. S. Patel and M. M. Hingorani, Biophys. J. **68**, 186 (1995).
[29]J. Yu, T. Ha, and K. Schulten, Biophys. J. **93**, 3783 (2007).
[30]P. Soultanas, M. S. Dillingham, S. S. Velankar, and D. B. Wigley, J. Mol. Biol. **290**, 137 (1999).
[31]K. J. Moore and T. M. Lohman, Biophys. J. **68**, 180 (1995).
[32]T. M. Lohman and K. P. Bjornson, Annu. Rev. Biochem. **65**, 169 (1996).
[33]H. Y. Wang, T. Elston, A. Mogilner, and G. Oster, Biophys. J. **74**, 1186 (1998).
[34]H. M. Berman, J. Westbrook, Z. Feng, G. Gilliland, T. N. Bhat, H. Weissig, I. N. Shindyalov, and P. E. Bourne, Nucleic Acids Res. **28**, 235 (2000).
[35]M. Karplus and J. A. McCammon, Nat. Struct. Biol. **9**, 646 (2002).
[36]See supplementary material at http://dx.doi.org/10.1063/1.4739308 for (a) complete details of all motor proteins investigated with the corresponding nucleotides in their enzymatic pocket; and (b) further information concerning the coordinating dynamics of Mg^{2+} with ATP.
[37]W. Humphrey, A. Dalke, and K. Schulten, J. Mol. Graphics **14**, 33 (1996).
[38]C. R. Woese, Proc. Natl. Acad. Sci. U.S.A. **54**, 71 (1965).
[39]L. Kale, R. Skeel, M. Bhandarkar, R. Brunner, A. Gursoy, N. Krawetz, J. Phillips, A. Shinozaki, K. Varadarajan, and K. Schulten, J. Comput. Phys. **151**, 283 (1999).
[40]J. C. Phillips, R. Braun, W. Wang, J. Gumbart, E. Tajkhorshid, E. Villa, C. Chipot, R. D. Skeel, L. Kale, and K. Schulten, J. Comput. Chem. **26**, 1781 (2005).
[41]A. D. MacKerell, Jr., N. Banavali, and N. Foloppe, Biopolymers **56**, 257 (2000).
[42]N. Foloppe and A. D. MacKerell, J. Comput. Chem. **21**, 86 (2000).
[43]A. D. MacKerell, D. Bashford, M. Bellott, R. L. Dunbrack, J. D. Evanseck, M. J. Field, S. Fischer, J. Gao, H. Guo, S. Ha, D. Joseph-McCarthy, L. Kuchnir, K. Kuczera, F. T. K. Lau, C. Mattos, S. Michnick, T. Ngo, D. T. Nguyen, B. Prodhom, W. E. Reiher, B. Roux, M. Schlenkrich, J. C. Smith, R. Stote, J. Straub, M. Watanabe, J. Wiorkiewicz-Kuczera, D. Yin, and M. Karplus, J. Phys. Chem. B **102**, 3586 (1998).
[44]E. Bae and G. N. Phillips Jr., J. Biol. Chem. **280**, 30943 (2005).
[45]W. L. Jorgensen, J. Am. Chem. Soc. **103**, 335 (1981).
[46]W. C. Swope, H. C. Andersen, P. H. Berens, and K. R. Wilson, J. Chem. Phys. **76**, 637 (1982).
[47]J. C. Liao, S. Sun, D. Chandler, and G. Oster, Eur. Biophys. J. **33**, 29 (2004).